

## The mobility spatial distribution function: Turn-on dynamics of polymer photocells

Noam Rappaport, Olga Solomesch, and Nir Tessler<sup>a)</sup>

*Microelectronic and Nanoelectronic Centers, Electrical Engineering Department, Technion Israel Institute of Technology, Haifa 32000, Israel*

(Received 30 June 2005; accepted 31 January 2006; published online 28 March 2006)

To better understand the transport in thin film devices and the role of the excitation density we have measured the photocurrent dynamic response of a photocell upon the switch on of light excitation. Unlike the standard time of flight methods that utilize a pulse excitation we employ a step function that is more compatible with real device operating conditions. The fact that the steady state of the step function is the cw operation of the device allows us to examine the role of charge density and use device analysis tools. To explain the broadened features measured we introduce a physical scheme by which the dispersive nature is due to spatial inhomogeneity, and the semiconducting layer is considered to be comprised of a distribution of parallel pathways (on the nanometer scale) each having a different, but well defined, mobility value. This insight allows us to extract, in a unique way, a mobility distribution function. The mean values of this distribution function are in good agreement with those deduced by previous measurements made on the same sample in which the mobility was determined from the excitation power dependence of the photocurrent quantum efficiency. © 2006 American Institute of Physics. [DOI: 10.1063/1.2180435]

### INTRODUCTION

Transient transport measurements are many times conducted on specially designed configurations, the most popular of which is the pulsed excitation time of flight performed on micron-thick films.<sup>1,2</sup> It has been established that it is also important to conduct transient transport measurements on real device structures and under operating conditions that are as close as possible to normal device operating conditions. In the context of conjugated molecule based devices this has been performed using a light emitting diode (LED) configuration<sup>3-5</sup> as well as field effect transistors<sup>6</sup> (FETs) but not so much using a photocell device.<sup>7</sup> For device-configuration measurements one typically prefers the step function excitation which is common in electrical excitation schemes (LEDs and FETs) but not in photoexcitation schemes. In this paper we use step function photoexcitations with varying intensities to study the transport phenomena in organic photocell device configuration. Since the long-time limit of the step function is the cw case, this technique (unlike pulsed excitation) allows us to compare directly with cw power dependence measurements.<sup>8</sup>

Under quasiequilibrium conditions, a photocell made of a semiconductor with a well-defined (single value) mobility would produce in response to light excitation switch on a linearly rising current up to a final steady state value<sup>7</sup> (see Fig. 1). This response corresponds to the filling up of the layer with the charge specie which occurs with a time constant equivalent to the transport time across the device. After the charge front reaches the back contact, the layer is full of the charge specie and the photocurrent settles to its steady state value. In organic devices there would typically be a

large difference between the settling time of electrons and holes and hence at short times there would be a sharp step-like rise of the photocurrent due to the fast charge specie followed by a slow ideally linear slope due to the slower carriers. By measuring the rise time and knowing the layer thickness and the voltage drop one can evaluate the mobility of the slow carriers.

When using thin film devices one is often concerned with the possible occurrence of nonequilibrium conditions that, if present, would broaden the response in a manner that would make the mobility an ill-defined concept.<sup>9</sup> It has been shown that due to the disordered nature of organic materials, time of flight measurements performed on thin samples (below 1000 nm) would typically display a dispersive curve. It has been independently argued that a dispersive nature is typically due to energy relaxation that takes place during the charge transport and can take up to several microns.<sup>1,9,10</sup> In such a case, of continuous relaxation, the notion of mobility is an ill-defined concept.<sup>9</sup> We propose here that in really thin

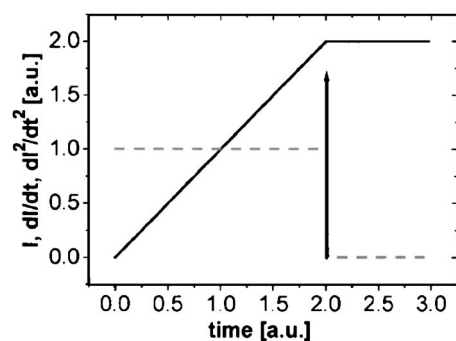


FIG. 1. Ideal photocurrent turn-on response for a device that consists of a layer with a single, well defined mobility. The solid line is the photocurrent, the dashed line is the first derivative of the photocurrent, and the spike is the inverse of the second derivative.

<sup>a)</sup>Electronic mail: nir@ee.technion.ac.il; URL: www.ee.technion.ac.il/orgelect

devices (below  $\sim 300$  nm) the dispersive nature is not due to dynamic relaxation but rather due to inhomogeneous distribution of the transport properties across the thin film. This implies that the film is composed of many parallel pathways each having a time independent (i.e., well defined) mobility value. As we show below, the width of such filaments would be in the 30–100 nm range, making it undetectable by optical imaging systems (i.e., we are not discussing here the hot spots that would appear in ill-prepared devices but rather a phenomena that is on a much finer scale). The strength of the approach we introduce here is that we can now analyze the transport using standard equations and extract the statistical distribution of the transport properties directly from the measured response. We deduce the average mobility value and use it to compare with other measurement techniques we have performed on the same device.

## EXPERIMENTAL DETAILS

A device was fabricated by spin coating a solution of poly[2-methoxy-5-(2-ethylhexyloxy)-1,4-phenylenevinylene] (MEH-PPV) in toluene on a glass substrate with an indium tin oxide (ITO) layer additionally covered with a spin coated aqueous dispersion of poly(3,4-ethylenedioxythiophene) poly(styrenesulfonate) (PEDOT) layer. The layers were annealed in a vacuum oven followed by evaporation of an aluminum back contact. The layer thickness was approximately 300 nm. The device was placed in front of an opening in an integrating sphere (Labsphere IS-040-SL) that was fed by a LED with a peak intensity at 505 nm (Lumileds LXHL-ME1D). The integrating sphere was equipped with a calibrated Si detector for monitoring the steady state light intensity. The LED was driven by an Agilent 8114A pulse generator in current mode triggered by a low frequency signal generator. The photocurrent was monitored using a Femto DLPCA-200 transimpedance amplifier feeding a digital Tektronix oscilloscope. The built-in potential of the device was measured as the saturation value for the open circuit voltage under high intensity illumination. This value was approximately  $-1$  V.

## RESULTS AND DISCUSSION

### Transient measurements

Since the step function excitation is not common in optical excitation time of flight measurements we start with the basic features of an ideal measurement.<sup>7</sup> The step function creates a charge front that moves into the device and fills it with charge. During this filling process the photocurrent rises and it reaches a plateau once the device is full (the charge front has reached the other end). For a single mobility value (a  $\delta$ -function type of mobility distribution) the current would ideally rise at a constant rate, proportional to the mobility value, towards steady state where the photocurrent response levels off (see Fig. 1). For this case, the second derivative with time of the response would produce a spike at the point of time where the photocurrent levels off. This point of time is inversely proportional to the mobility value and can be used to deduce it.

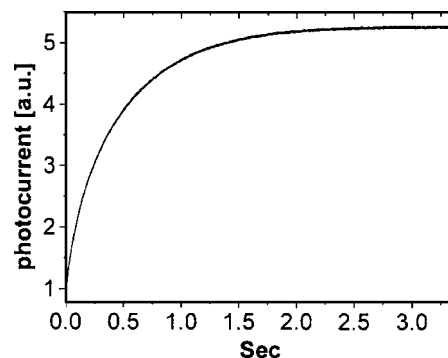


FIG. 2. Measured photocurrent transient response of the MEH-PPV device at low excitation intensity and 0 V applied bias (short circuit).

Figure 2 shows a typical photocurrent transient response to a low-level excitation of a thin (300 nm) film device. The applied bias was 0 V (short circuit), which means that the driving voltage was that of the built-in potential only, i.e., 1 V.

The basic features of the measured transient response (Fig. 2) include a sharp increase in the current that is due to the fast hole-current buildup, followed by a slow rise of the electron current up to its steady state value. The gradual process of the current buildup is the result of the carrier concentration buildup within the active layer as the carriers are swept from their place of generation towards their respective contacts and charge the device (see details in Ref. 8). In principle, knowing the layer thickness and measuring the transient time may serve us in calculating the mobility. As was discussed above, for a device that can be characterized by a well-defined, single value, mobility the slow increase in the current is basically linear (Fig. 1), making it simple to deduce the point at which the transient ends. In our case, as can be seen in Fig. 2, the transient for the electron current lacks a clear single slope by which the end of transient or time of flight of the electrons may be inferred. Instead we find a transient with a dispersive nature from which it is impossible to pinpoint a single value for the time of flight or the mobility.

The lack of a clear linear slope in the response shown in Fig. 2 is equivalent to a lack of a plateau in classical, pulsed excitation, time-of-flight (TOF) measurements (typically performed on micron thick devices). Such “anomaly” has been discussed many times in the past in the context of dispersive transport,<sup>9,10</sup> where the effective mobility is said to vary as a function of time due to nonequilibrium time domain trapping, detrapping, and hopping of the traversing charges. The mobility is said to be an ill-defined concept.<sup>9</sup> We propose here an alternative physical picture for describing the above transient behavior that we believe is better suited for thin film devices (i.e., well below  $1 \mu\text{m}$ ). We argue that the electronic disorder present in such films gives rise to a distribution of parallel pathways each having a well defined mobility value. Each pathway displays the response shown in Fig. 1 as we assume quasiequilibrium transport (well defined mobility) for each pathway. The ever-changing slope is now explained as a result from each path reaching its steady state at a different point in time due to a different mobility value.

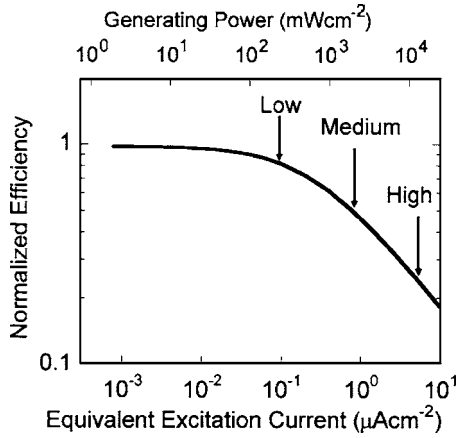


FIG. 3. Graph of the quantum efficiency vs excitation density for the sample at 0 V bias with indications to the densities at which the measurements of Fig. 4 were taken (from Ref. 8).

The fact that the layer is very thin in the direction of transport provides us with the reasoning to assume that on such a scale there would be mesoscopic spatial heterogeneity in the packing of the energy states and their relative distance that can be depicted as a parallel distribution of mobilities.

To understand why this feature is unique to thin film devices we examine the classical form of charge-packet propagation under electric field:  $p(x,t) \propto \exp[-(x - \mu Et)^2 / 4D_t]$  from this expression one can deduce the width of the packet after propagating the length of the device:  $\Delta X = \sqrt{L^2 / V \sqrt{D} / \mu} \propto \sqrt{L^2 (\eta \cdot 0.026) / V}$ . Here  $L$  is the length of the device and  $\eta$  is the enhancement of the Einstein relation<sup>11,12</sup> found in disordered materials. Assuming  $L = 300$  nm,  $V = 2$  V, and letting  $\eta$  vary between 1 and 4 we find that a carrier will sample to the side with a maximum of 34–136 nm. The maximum volume a carrier samples while crossing the device is of the order of  $100 \times 100 \times 300$  nm<sup>3</sup>, which is far too small to reproduce the broad density of states typical of disordered media. Different spots across the sample will present a slightly different effective density of states (DOS) function and hence will be associated with a slightly different mobility value. We note that the distribution we describe here is very fine in space (nanometer scale) and is not related to the hot spot phenomena that can be observed using optical imaging devices. We have verified this intuitive picture using Monte Carlo simulation of hopping transport which will be reported elsewhere.

The physical picture arising from such a description is that each mobility pathway that reaches its steady state stops contributing to the rise in current and thus we get a monotonically decreasing slope. Mathematically the formula describing this process is

$$J_e(t) = APq \left\{ \int_{d^2/Vt}^{\infty} g(\mu_e) d\mu_e + \int_0^{d^2/Vt} g(\mu_e) \frac{t}{t_{tr}(\mu_e)} d\mu_e \right\}, \quad (1)$$

where  $J_e$  is the electron current density,  $g(\mu_e)$  is the mobility distribution function (MDF) for the electron pathways,  $t_{tr}(\mu_e)$  is the transit time across the device for an electron with mobility  $\mu_e$  [ $t_{tr}(\mu_e) = d^2 / \mu_e V$ ],  $d$  is the device thickness,

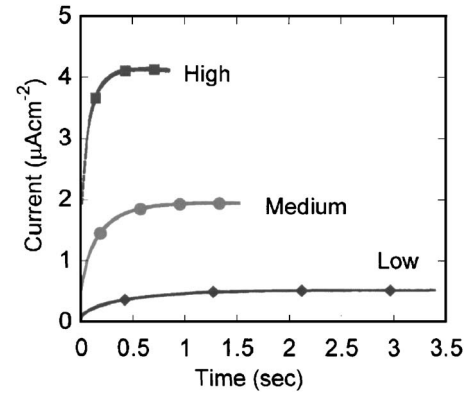


FIG. 4. Measured photocurrent transient in response to a step function excitation. The three different excitation powers used here correspond to those marked on Fig. 3.

$q$  is the electron charge,  $P$  is the incident light intensity, and  $A$  is the carrier pair generation efficiency (number of electron-hole pairs generated per unit of incident intensity). The first term in the brackets represents the pathways that have reached their steady state by time  $t$  while the second term is for those that have not. The ideal response shown in Fig. 1 is reproduced by Eq. (1) if we let  $g(\mu_e)$  to be a delta function (single mobility value).

To describe the data presented in Fig. 2 with the aid of Eq. (1) one has to find a proper expression for the MDF,  $g(\mu_e)$ . This is somewhat similar to finding a proper waiting time distribution (WTD) function.<sup>9,10</sup> Drawing on the studies performed in the context of time domain distribution we can state that just as the functional form of the time domain distribution function (WTD) is dependent on the actual density of states<sup>13–15</sup> so would the spatial domain distribution (MDF). In the absence of the correct shape for the DOS we cannot attempt to derive theoretically the MDF  $g(\mu_e)$ . However, as we show below, the simple form of Eq. (1) allows us to extract the MDF from the measured data (Fig. 2).

To extract the mobility distribution function we first re-examine the physical picture that has just been proposed. Pathways that have already reached their steady state cease to contribute to the first derivative of the current and those pathways that have not yet reached their steady state contribute a constant value to the first derivative over time (proportional to the local mobility value). The rate of change of the first derivative (i.e., the second derivative) should therefore be an indication as to the relative weight of the mobility pathway that has just reached its steady state. The mobility distribution function should therefore be deduced by examining the second derivative of the measured photocurrent or the second derivative of Eq. (1). Indeed, using Eq. (1) we can find an explicit expression for the mobility distribution as is shown in Eq. (2).

$$\frac{d^2 J(t)}{dt^2} = -\frac{APqd^2}{2Vt^3} g\left(\frac{d^2}{Vt}\right). \quad (2)$$

The result given in Eq. (2) is central to this paper as it provides analytical means to extract the mobility distribution function directly from the measured data. Having established

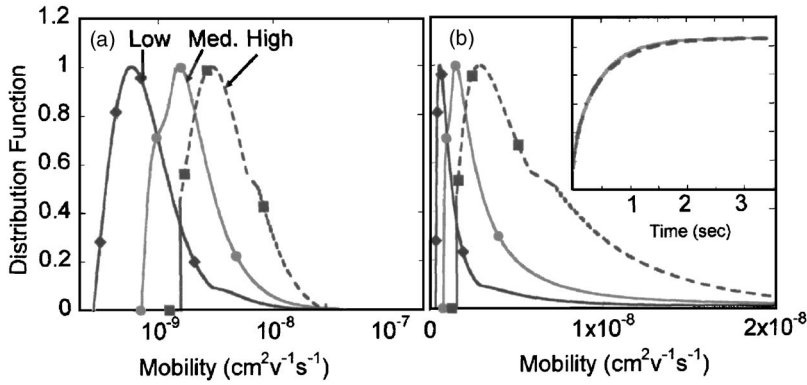


FIG. 5. The mobility distribution functions,  $g(\mu)$ , for the low (diamonds), medium (circles), and high (squares) excitation intensities. (a) The mobility scale is logarithmic. (b) The mobility scale is linear. The inset shows the measured time response of the low power excitation (dashed) and of the same response as reproduced using Eq. (1) and the extracted  $g(\mu)$  (solid).

the framework we move to analyzing current transients at different excitation powers. To be able to relate the data reported here to that reported in Ref. 8 we plot in Fig. 3 the measurement of the quantum efficiency versus excitation density at 0 V bias from Ref. 8. The arrows in Fig. 3 indicate the power levels used here. We note that we are able to directly compare the cw and transient measurements only due to our use of a step function excitation rather than a short pulse.

In Fig. 4 we present the measured photocurrent transients in response to a step function excitation. The step function height was varied among low (diamonds), medium (circles), and high (squares) intensities. The definitions of low, medium, and high are with respect to the power dependence of the photocurrent efficiency (see Fig. 3). Following the detailed discussion in Ref. 8 the high excitation density is affected by space charge effects that are not included in Eq. (1) hence, in the following analysis, one should remember that the shape of the MDF at high excitation density may not be as accurate as the medium and low ones.

Figure 5 shows the mobility distribution functions that were obtained by applying Eq. (2) to the data in Fig. 4 and Table I collates the relevant parameters. We find that the average mobility value systematically increases as a function of excitation density which is in qualitative agreement with the trends reported for hole transport for the same material in FET device configuration.<sup>15,16</sup> At the high power range the deduced average mobility is about three times smaller than the value reported in Ref. 8 [ $10^{-8} \text{ cm}^2/(\text{V s})$ ], which was deduced from the power dependence of the photocurrent quantum efficiency using the same device. Since the analysis in Ref. 8 did not account for the presence of different paths (or a mobility distribution function) and the relatively large

variance (see Table I) found in these MEH-PPV films, we consider the values reported here to be in qualitatively good agreement with those in Ref. 8.

Also shown in Table I are the MDF standard deviations and its ratio to the average mobility. We note that as the power density (charge density) goes up the mobility becomes better defined as the relative  $\sigma$  to average mobility ratio is reduced. We believe that this is due to filling up and saturation of the slow mobility pathways which is somewhat equivalent to trap filling.

## CONCLUSIONS

To better understand the transport in organic and molecular thin film devices we performed transient response measurements on the same sample that was used in Ref. 8. We have introduced a concept that enables understanding and analyzing dispersivelike transport, namely, the MDF. Unlike the time domain distribution function the concept of spatial domain mobility distribution is relatively simple and more intuitive for the case of thin (submicron) devices. Most importantly, a direct method for extracting the MDF was developed and implemented (Fig. 5). We found qualitatively good agreement between the average mobility value and the values deduced by the cw power dependent method.<sup>8</sup> We attribute this good agreement to the device-oriented physical picture that is behind the model used here. We believe that the rigorous treatment of the spatial homogeneity opens the possibility to extend this picture and account for inhomogeneity in the contact phenomena to explain the unique temperature dependence found in contact with disordered materials.

Another way of looking at the physical picture introduced here is that the expected filamentary nature of charge motion through a disordered material creates a statistics of filament lengths and traversal durations that can be viewed upon as being grouped into a distribution of pathways with different mobility values. We believe that a broad distribution of mobility values (nanoscale filaments) may significantly contribute to device degradation as some of the molecules undergo excessive oxidation/reduction processes which is the essence of charge hopping. Since the shape and width of the distribution are dependent on the electronic properties of the film, the method presented here can serve as an optimization tool for material development.

TABLE I. Average mobilities, MDF standard deviation, and the standard deviation to average mobility ratio extracted using the mobility distribution model for different excitations.

| Intensity | $\mu_e$ (average)<br>[ $\text{cm}^2/(\text{V s})$ ] | MDF standard<br>deviation $\sigma$<br>[ $\text{cm}^2/(\text{V s})$ ] | $\sigma/\mu_e$ |
|-----------|---|--|----------------|
| Low       | $6.65 \times 10^{-10}$                              | $5.4 \times 10^{-10}$  | 0.81           |
| Medium    | $1.6 \times 10^{-9}$                                | $1.1 \times 10^{-9}$   | 0.69           |
| High      | $3.2 \times 10^{-9}$                                | $1.95 \times 10^{-9}$  | 0.61           |

## ACKNOWLEDGMENTS

The authors acknowledge support by the Israel Science Foundation. One of the authors (O.S.) expresses deep gratitude to the Center of Absorption in Science, Ministry of Absorption, Israel.

<sup>1</sup>M. Van der Auweraer, F. C. Deschryver, P. M. Borsenberger, and H. Bassler, *Adv. Mater. (Weinheim, Ger.)* **6**, 199 (1994).

<sup>2</sup>A. J. Campbell, D. D. C. Bradley, and H. Antoniadis, *Appl. Phys. Lett.* **79**, 2133 (2001).

<sup>3</sup>D. J. Pinner, R. H. Friend, and N. Tessler, *J. Appl. Phys.* **86**, 5116 (1999).

<sup>4</sup>A. J. Campbell, D. D. C. Bradley, H. Antoniadis, M. Inbasekaran, W. S. Wu, and E. P. Woo, *Appl. Phys. Lett.* **76**, 1734 (2000).

<sup>5</sup>D. Braun, D. Moses, C. Zhang, and A. J. Heeger, *Appl. Phys. Lett.* **61**, 3092 (1992).

<sup>6</sup>Y. Roichman and N. Tessler, *Turn-on and Charge Build-up Dynamics in*

*Polymer Field Effect Transistors*, *Mater. Res. Soc. Symp. Proc.* **871E**, I4.5 (2005).

<sup>7</sup>N. Marc, J. Y. Moisan, N. Wolffer, B. Andre, and R. Lever, *Philos. Mag. B* **74**, 81 (1996).

<sup>8</sup>N. Tessler and N. Rappaport, *J. Appl. Phys.* **96**, 1083 (2004).

<sup>9</sup>H. Scher and E. M. Montroll, *Phys. Rev. B* **12**, 2455 (1975).

<sup>10</sup>H. Scher, M. F. Shlesinger, and J. T. Bendler, *Phys. Today* **44**(1), 26 (1991).

<sup>11</sup>Y. Roichman and N. Tessler, *Appl. Phys. Lett.* **80**, 1948 (2002).

<sup>12</sup>N. Tessler and Y. Roichman, *Org. Geochem.* **6**, 200 (2005).

<sup>13</sup>B. Hartenstein, H. Bassler, A. Jakobs, and K. W. Kehr, *Phys. Rev. B* **54**, 8574 (1996).

<sup>14</sup>W. Geens, S. E. Shaheen, B. Wessling, C. J. Brabec, J. Poortmans, and N. S. Sariciftci, *Org. Electron.* **3**, 105 (2002).

<sup>15</sup>S. Shaked, S. Tal, Y. Roichman, A. Razin, S. Xiao, Y. Eichen, and N. Tessler, *Adv. Mater. (Weinheim, Ger.)* **15**, 913 (2003).

<sup>16</sup>Y. Roichman, Y. Preezant, and N. Tessler, *Phys. Status Solidi A* **201**, 1246 (2004).